TASK QUARTERLY 6 No 4 (2002), 609–620

DIMENSIONING AND PERFORMANCE ANALYSIS OF AN AXIAL HYDRAULIC TURBINE OF HIGH POWER/WEIGHT RATIO

FRANK KENYERY[1], ROBERT REY[2] AND RICARDO NOGUERA[2]

[1] *Universidad Simón Bolívar,*
Departamento de Conversión y Transporte de Energia,
Apartado Postal N° 89.000, Caracas 1080-A, Venezuela
fkenyery@usb.ve

[2] *Ecole Nationale Superieure D'Arts et Metiers,*
151, boulevard de l'Hôpital, Paris 75013, France

(Received 30 August 2001; revised manuscript received 15 July 2002)

Abstract: The purpose of this research is to develop a methodology for dimensioning and performance analysis of a stage of Hydraulic Axial-Flow Turbines of High Power to Weight Ratio (HAFT-HPWR).

The HAFT-HPWR consists of two rows (stator and rotor) with non-twisted blades. The axial flow turbine of higher power to weight ratio is that with a degree of reaction equal to zero.

The experimental results on a single stage 50% reaction turbine show a big influence of Reynolds number on the turbine performance. The zone of operation at the best efficiency point varies strongly with the rotation speed.

The performance analysis of HAFT-HPWR requires the precise assessment of the influence of the Reynolds number on deflection and the hydraulic losses. Due to complexity of the flow in an axial turbine, such assessment should be based on 3D numerical simulation, in order to compute the hydraulic losses present in a stage of HAFT-HPWR, without using models and correlations.

Keywords: hydraulics, axial flow turbine performance, cavitation

Nomenclature

ρ	fluid density
ν	cinematic viscosity
s	pitch
c	chord
H	head
H_{th}	theoretical head
n	rotation speed [rpm]
$\omega = 2\pi n/60$	angular speed [rad/s]
$\Phi = C_a/U_m$	flow coefficient
$\Psi = gH/U_m^2$	head coefficient
$\Psi_{\mathrm{th}} = gH_{\mathrm{th}}/U_m^2$	theoretical head coefficient
$Q = \pi/2 \cdot \omega \cdot D_m^3 \delta \cdot \Phi/\eta_v$	flow-rate

τ	radial clearance
$\Psi_p = g \cdot H/U_p^2$	head coefficient at the rotor periphery
$R = (W_2^2 - W_3^2)/(2gH_{\rm th})$	degree of reaction
θ_c	profile camber angle
t_{TE}	trailing edge thickness
$\eta_h = H_{\rm th}/H$	hydraulic efficiency
$\eta = P_{\rm output}/(\rho g Q H)$	global efficiency
η_v	volumetric efficiency
$D_{F_{\rm stator}} = 1 - C_2/C_{\max}$	stator diffusion factor
$D_{F_{\rm rotor}} = 1 - W_3/W_{\max}$	rotor diffusion factor
$\zeta_{U_S} = \Delta p_{oS}/(\rho \cdot U_m^2)$	stator hydraulic loss coefficient
$\zeta_{U_R} = \Delta p_{oR}/(\rho \cdot U_m^2)$	rotor hydraulic loss coefficient
$\zeta_2 = \Delta p_o/(\rho \cdot C_2^2)$	cascade loss coefficient
$\zeta_{\rm sec}$	secondary loss coefficient
$\zeta_{\rm cl}$	clearance loss coefficient
β_m	mean flow relative angle
$\mathrm{Re}_c = \rho \cdot C \cdot c/\mu$	Reynolds number
U_m	blade speed at the mean diameter

1. Introduction

In the oil industry, multiphase and down-hole pumps require a variable speed driver with high power output, small size and high regulation capacity [1].

A Low Specific Speed Hydraulic Axial Flow Turbine (LSHAFT) is a driver machine having these characteristics, since it has a high head coefficient and a high flow coefficient. A high head coefficient implies a small size turbine, and a high flow coefficient implies a high power output turbine. According to Figure 1, low specific speed hydraulic axial flow turbines have higher values of flow coefficients and head coefficients than classic hydraulic turbines (Pelton, Francis and Kaplan).

A single stage LSHAFT with non-twisted blades and constant cross-sectional area (Figure 2) is a very simple machine to build with a CNC machine tool; the blade shape can be machined down directly on the periphery of a metal disc.

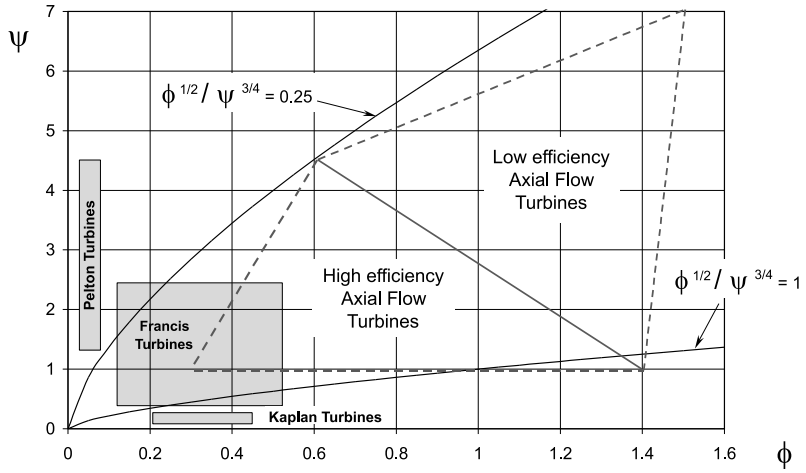

Figure 1. Head coefficients and flow coefficients for various types of turbine (Horlock 1966) [2]

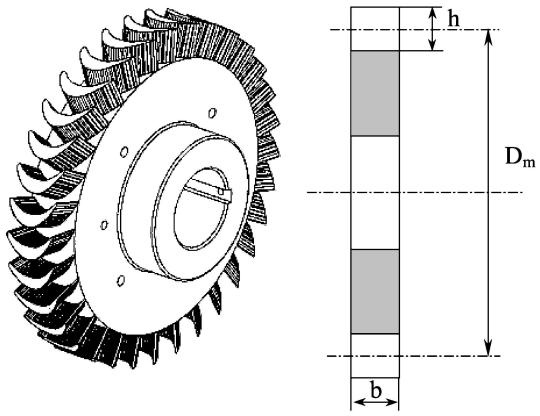

Figure 2. Main dimensions of a LSHAFT rotor with short non-twisting blades

The purpose of the present work is to develop a methodology for dimensioning and analyzing the performance of HAFT-HPWR. The bibliography of HAFT-HPWR is very limited. Most of the papers dealing with LSHAFT are related to steam and gas turbines [3–5]. As it is used for thermal turbines, the dimensioning and performance analysis of a HAFT-HPWR stage is based on two dimensionless parameters: the flow coefficient, Φ, and the theoretical head coefficient, $\Psi_{\rm th}$.

Cavitation is an important phenomenon in hydraulic turbines. The design methodology should include the blade profile selection in order to avoid a turbine with a high critical NPSH value.

The stage turbine design and performance analysis should therefore cover three main aspects: a) selection of design duty coefficients (Φ, $\Psi_{\rm th}$), b) design of the velocity triangle, and c) the fluid flow considerations (efficiency, losses, cavitation and blade profile selection).

The dimensionless parameters (Φ, $\Psi_{\rm th}$) are selected so that the utilization factor ξ of the whole turbine is maximized. In this way, it is possible to reduce the hydraulic energy supplied to the turbine. Therefore, the utilization factor ξ is defined as:

$$\xi = \frac{H_{\rm utilized}}{H_{\rm available}} = \frac{H}{H + C_3^2/2g}. \tag{1}$$

In the absence of fluid friction, the utilization factor ξ is written as:

$$\xi = H_{\rm th}/(H_{\rm th} + C_3^2/2g). \tag{2}$$

2. Stage dimensioning

2.1. Configuration of an axial-flow turbine stage

An axial-flow turbine stage is composed of a stator followed by a rotor. Figure 3a establishes the morphology of a classic stage of an axial-flow turbine; the stator is represented by a stationary rectilinear cascade of blades and the rotor by a rectilinear cascade moving downwards with U velocity. The velocity triangles can be made dimensionless by dividing all velocities by the blade peripheral velocity U. The dimensionless velocity triangles of an axial turbine stage for $\alpha_1 = 0^\circ$ are shown in Figure 3b.

From the dimensionless velocity triangles and the assumption of a constant flow angle α_2 (stator with short and non-twisted blades), it can be shown that the maximum utilization factor $\xi_{\max}$ is obtained for the following duty coefficients:

$$\Phi = 2 \cdot (1 - R) / \tan\alpha_2 \tag{3}$$

and

$$\Psi_{\text{th}} = 2 \cdot (1 - R). \tag{4}$$

In the preceding equations, the parameter R is the degree of reaction of the turbine stage. The maximum utilization factor is given by:

$$\xi_{\max} = 1/(1 + 2 \cdot (1 - R)/\tan\alpha_2). \tag{5}$$

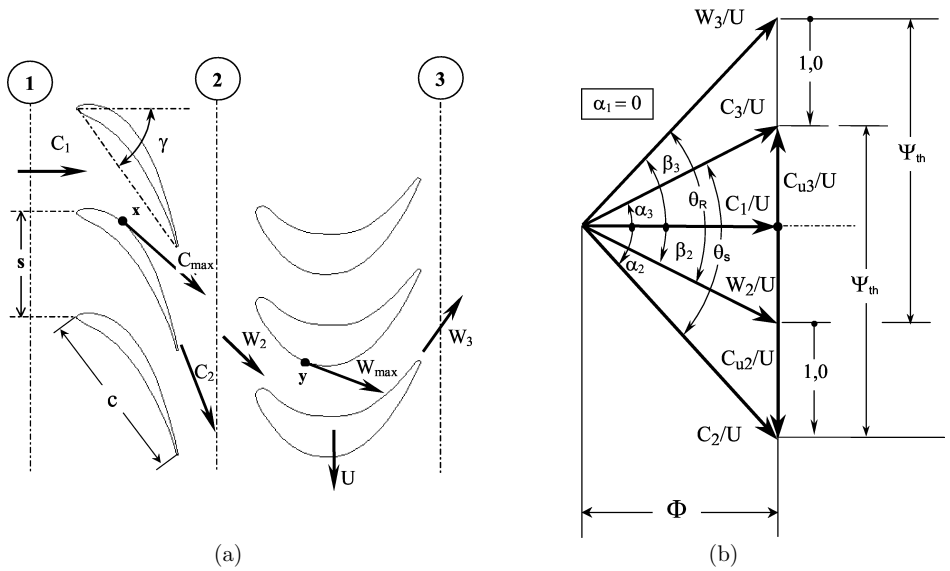

Figure 3. (a) An axial-flow turbine stage; (b) dimensionless velocity triangles of an axial turbine stage with constant axial velocity

For a flow angle $\alpha_2 = 73.9^\circ$ and different degrees of reaction, the obtained dimensionless coefficients are presented in Table 1.

Table 1. Dimensionless coefficients, $\alpha_2 = 73.9^\circ$

	$R = 0$	$R = 0.5$	$R = 0.75$
$\xi_{\max}$	0.634	0.776	0.874
Φ	0.577	0.289	0.144
Ψ_{th}	2	1	0.5

2.2. Specific speed and specific diameter

The relative span (blade aspect ratio) $\delta = h/D_m$ is an important dimensionless geometric parameter for LSHAFT with non-twisted blades. In practice, a maximum value of 0.15 for the relative span is accepted. Beyond this maximum value, the radial

equilibrium flow condition is not fulfilled and also a high incidence loss on the blade can occur.

The turbine performance and size can well be determined from the dimensionless specific speed Ω and the specific diameter Λ:

$$\Omega = \frac{\omega\sqrt{Q}}{(gH)^{3/4}} = 2\sqrt{\pi}\frac{\eta_h^{3/4}}{\eta_v^{1/2}}\frac{\Phi^{1/2}}{\Psi_{\rm th}^{3/4}}\cdot\delta^{1/2}, \tag{6}$$

$$\Lambda = \frac{D_m(gH)^{1/4}}{\sqrt{Q}} = \frac{1}{\sqrt{\pi}}\frac{\eta_v^{1/2}}{\eta_h^{1/4}}\frac{\Psi_{\rm th}^{1/4}}{\Phi^{1/2}}\cdot\delta^{-1/2}. \tag{7}$$

Figure 4 shows the relationship between the specific speed Ω and specific diameter Λ for axial-flow turbines with $\alpha_2 = 73.9^\circ$ and different degrees of reaction ($R = 0$ and $R = 0.5$). This diagram was constructed assuming ideal conditions ($\eta_h = 1$, $\eta_v = 1$) and varying δ from 0 to 1. For an action turbine ($R = 0$), the values $\Psi_{\rm th} = 2$ and $\Phi = 0.577$ were taken, while $\Psi_{\rm th} = 1$ and $\Phi = 0.289$ were selected for the 50% reaction turbine. Figure 4 also shows that an action turbine is the smallest size turbine for a given specific speed.

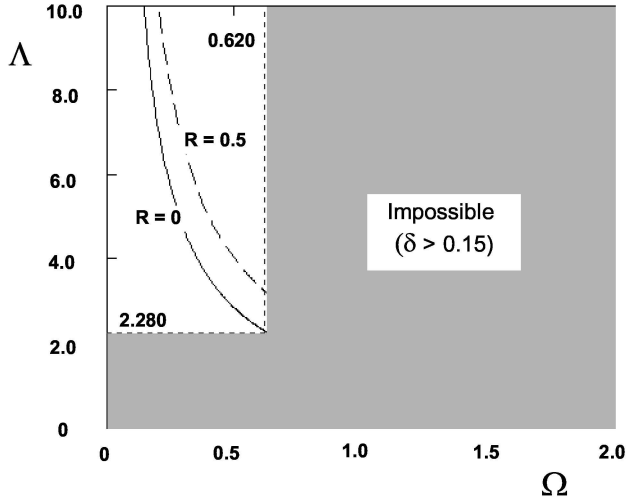

Figure 4. Relation between the specific speed Ω and the specific diameter Λ, for $\alpha_2 = 73.9^\circ$ and different R

Therefore, for $\delta = 0.15$, the smallest turbine with non-twisted blades would be an action turbine with a specific diameter $\Lambda = 2.28$, and a specific speed $\Omega = 0.62$.

2.3. Dimensioning in cavitation regime

If cavitation were not considered in the HAFT-HPWR dimensioning, the resulting turbine would require a high back-pressure in the exit conduct, which could also decreases the available head.

In a cascade, a low-pressure zone occurs where the liquid reaches its maximum speed. The cascade diffusion factor D_F is an important design parameter to avoid cavitation in turbomachines.

The required theoretical cavitation number is defined as:

$$\sigma^* = \mathrm{NPSH}_{\mathrm{required}}/H_{\mathrm{th}}. \tag{8}$$

In the absence of fluid friction, the respective cavitation numbers for the stator and the rotor blade cascade are expressed as follow:

$$\sigma^*_{\mathrm{stator}} = \frac{1}{2\Psi_{\mathrm{th}}}\left\{\frac{C_3^2}{U_m^2} + \frac{C_2^2}{U_m^2}\left[\frac{1}{(1-D_{F_{\mathrm{stator}}})^2} - 1\right]\right\} - R, \tag{9}$$

$$\sigma^*_{\mathrm{rotor}} = \frac{1}{2\Psi_{\mathrm{th}}}\left\{\frac{C_3^2}{U_m^2} + \frac{W_3^2}{U_m^2}\left[\frac{1}{(1-D_{F_{\mathrm{rotor}}})^2} - 1\right]\right\}. \tag{10}$$

From these expressions it is observed that for a reaction stage, cavitation first occurs at the rotor, while for an action stage cavitation begins at the stator. By definition, the cavitation specific speed S and the cavitation specific diameter Λ_S are written as:

$$S = \omega\sqrt{Q}/(g\cdot\mathrm{NPSH})^{3/4} = \Omega/{\sigma^*}^{3/4}, \tag{11}$$

$$\Lambda_S = D_m(g\cdot\mathrm{NPSH})^{1/4}/\sqrt{Q} = {\sigma^*}^{1/4}\Lambda. \tag{12}$$

Figure 5 shows the variation of S and Λ_S as a function of the relative span δ for different R values and $D_F = 0.25$. In this figure, S and Λ_S were obtained using the expression for $\sigma^*_{\mathrm{stator}}$, $\Psi_{\mathrm{th}} = 2$ and $\Phi = 0.577$ for the action turbine, and the expression for $\sigma^*_{\mathrm{rotor}}$, $\Psi_{\mathrm{th}} = 1$ and $\Phi = 0.289$ for the 50% reaction turbine.

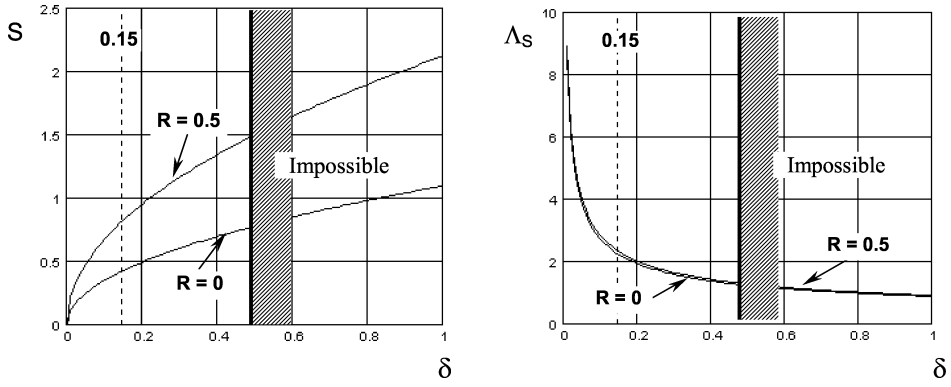

Figure 5. Variation the cavitation specific speed of S and the cavitation specific diameter Λ_S with the relative span δ ($F_D = 0.25$)

The cavitation dimensioning of a HAFT-HPWR from these last two figures indicates that:

1. For the same relative span δ, the fastest turbine is the one with 50% degree of reaction.
2. For the same rotation speed, a 50% reaction turbine requires a smaller NPSH value.
3. An action turbine and a 50% reaction turbine have the same size (same cavitation specific diameter Λ_S).

3. Selection of blade profile

The blade solidity (chord-pitch ratio) c/s determines the fluid acceleration and deflection occurring in the cascade. In order to get a small size turbine, the cascade

solidity should be selected such that the smallest diffusion factor D_F is obtained. D_F varies with the cascade blade parameters (solidity, stagger angle γ) and the selected blade profile (relative thickness, camber, *etc.*).

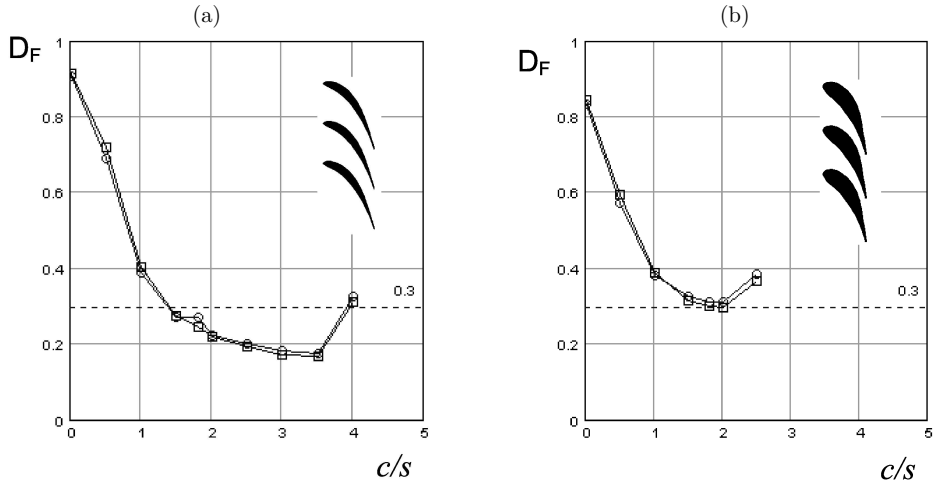

Figure 6. Variation of the diffusion factor with the blade solidity, NACA A3K7 profile primary series, $\theta_c = 80^\circ$, $\alpha_1 = 0^\circ$; (a) $t/c = 10\%$ relative thickness, (b) $t/c = 20\%$; ⊖⊖⊖ $\gamma = -54^\circ$, ⊟⊟⊟ $\gamma = -60^\circ$

NACA A3K7 profiles (primary series) were analyzed to determine the effect of blade solidity and profile relative thickness on the diffusion factor. Figure 6 shows the diffusion factor as a function of blade solidity for different stagger angles and profile relative thickness t/c of 10% (Figure 6a) and 20% (Figure 6b). Those D_F values were calculated using the source-vortex panel method [6, 7]. A very low diffusion factor ($D_F = 0.2$) can be achieved for solidities $c/s > 2$ and proper profile relative thickness.

4. 50% reaction turbine model

A single stage HAFT-HPWR model with a degree of reaction of 50% was design, built and tested (Figure 7). The stator and the rotor were machined down from two aluminum disks 18mm thick, and external diameter of 250mm. The non-twisted blades have 20mm height. The blade profile selected for the stator and rotor was a NACA A3K7 primary series $\theta_c = 79^\circ$. The stage geometric parameters are presented in Table 2.

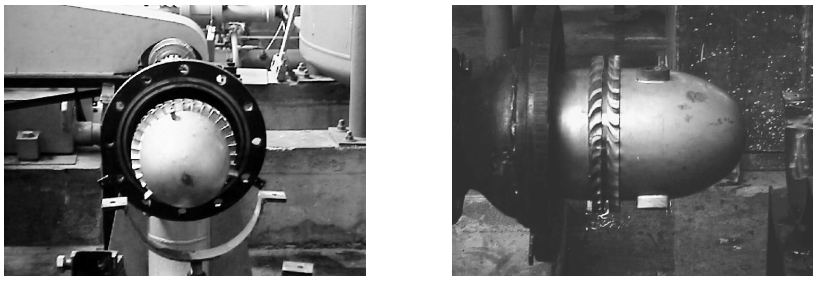

Figure 7. HAFT-HPWR model

Table 2. The stage geometric parameters

	Stator	Rotor
D_{tip}	250mm	250mm
D_m	230mm	230mm
D_{hub}	210mm	210mm
δ	0.087	0.087
c/s (at D_m)	1.150	1.114

	Stator	Rotor
Num. of blades	31	32
θ_c	79°	79°
γ	−48°	−48°
α_1	0°	—
α_2	60°	—

5. Experimental results

All tests were performed at the Mechanical Energy Conversion Laboratory of Universidad Simón Bolívar. The tests were carried out maintaining the $\text{NPSH}_{\text{available}}$ high enough to avoid cavitation. The head H was varied maintaining the rotation speed constant. In the tests, the rotation speed was varied from 500 to 1200rpm. For each operation point, the flow rate, torque, and static pressures at three locations:

1. stator inlet,
2. space between stator and rotor,
3. rotor outlet,

were measured. Also, the absolute velocity and flow angle were measured at the mean diameter D_m by two-dimensional probes (edge type) located at the three points mentioned above.

The variation of global efficiency η and hydraulic efficiency η_h with the flow coefficient is shown in Figure 8. These experimental results show a big influence of the rotation speed (Reynolds number) on the turbine performance. The zone of operation at the highest efficiency point varies strongly with the rotation speed.

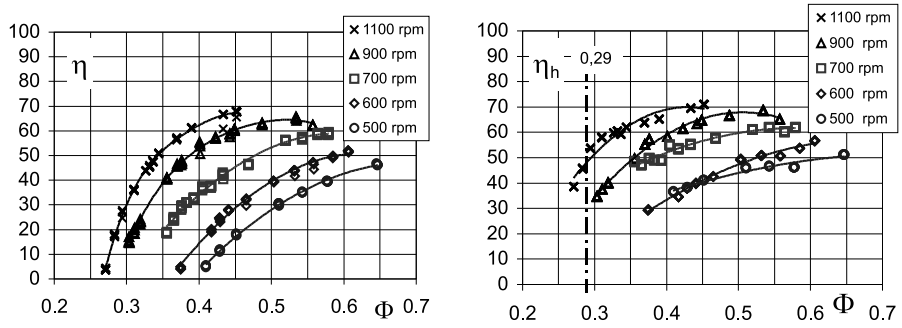

Figure 8. Hydraulic and global efficiency as a function of flow coefficient

6. HAFT-HPWR performances analysis

The performance analysis performed on the single stage HAFT-HPWR was dedicated, exclusively, to the hydraulic behavior. Indeed, the hydraulic losses represented 85% of the total losses as it was shown by the experimental results.

For a stage of a hydraulic turbine, the actual specific fluid energy transfer or head H is equal to the theoretical head plus the hydraulic losses:

$$H = H_{\text{th}} + z_h. \tag{13}$$

The hydraulic losses can be calculated from the stagnation pressure loss Δp_0 occurring at the stator and rotor:

$$z_h = (\Delta p_{0_S} + \Delta p_{0_R})/\rho g = (\zeta_{U_S} + \zeta_{U_R}) U_m^2/g. \tag{14}$$

The sources of hydraulic looses in the stator include the profile loss and the secondary flow losses. Additionally, the rotor hydraulic losses include the clearance loss.

The profile loss is a function of flow deflection θ and Reynolds number Re_c. It will be determined through a CFD numerical simulation of the flow field in an infinite rectilinear cascade, assuming a smooth blade surface (see Figure 9). The numerical code is the CFX 4.2 [8] which uses control volumes and the k-ε turbulence model.

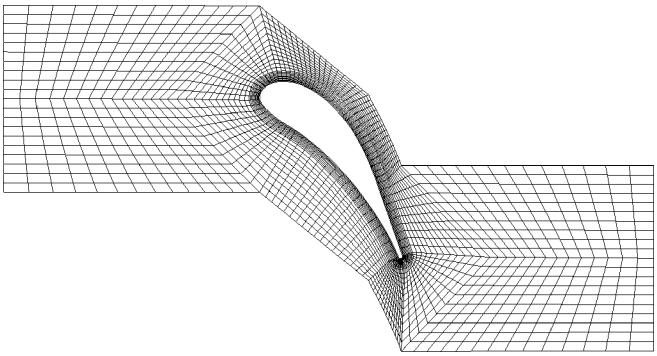

Figure 9. Cascade grid for the NACA profile A3K7 primary series $\theta_c = 79^\circ$, $t/c = 20\%$, $\gamma = -48^\circ$ and $c/s = 1.5$ (5696 elements)

From the numerical simulation results shown in Figure 10, the profile loss coefficient ζ_2 and flow deflection θ can be expressed as:

$$\zeta_2 = -8\cdot 10^{-10}\alpha_1^5 - 2\cdot 10^{-8}\alpha_1^4 - 7\cdot 10^{-7}\alpha_1^3 + 3\cdot 10^{-5}\alpha_1^2 + 5\cdot 10^{-4}\alpha_1 + 0.0777, \tag{15}$$

$$\theta = 0.9989\cdot\alpha_1 + 70.851, \tag{16}$$

or in terms of the Reynolds number as:

$$\zeta_2/\zeta_2^* = 1.0195(\text{Re}_\ell/10^5)^{-0.0948}, \tag{17}$$

$$\theta/\theta^* = 0.9996(\text{Re}_c/10^5)^{0.0052}, \tag{18}$$

where ζ_2^* and θ^* are the values corresponding to $\text{Re}_c = 10^5$.

The cascade secondary loss coefficient ζ_{sec} can be determined using the expression developed by Sharma-Butler [3, 9]:

$$\zeta_{\text{sec}} = \zeta_p \cdot \left(1 + \frac{4\pi\theta/180}{\sqrt{C_2/C_1}}\right) \cdot \frac{s\cdot\cos(\alpha_2) - t_{TE}}{h}. \tag{19}$$

From a relationship developed by Lakshminarayana [3], the clearance loss coefficient can be expressed by:

$$\zeta_{cl} = \frac{\Delta p_{o_{cl}}}{\rho U_p^2} = \frac{0.7\cdot\Psi_p^2\cdot\tau/h}{\cos\beta_m}\left[1 + 10\sqrt{\frac{\Phi}{\Psi_p}\frac{\tau/c}{\cos\beta_m}}\right]. \tag{20}$$

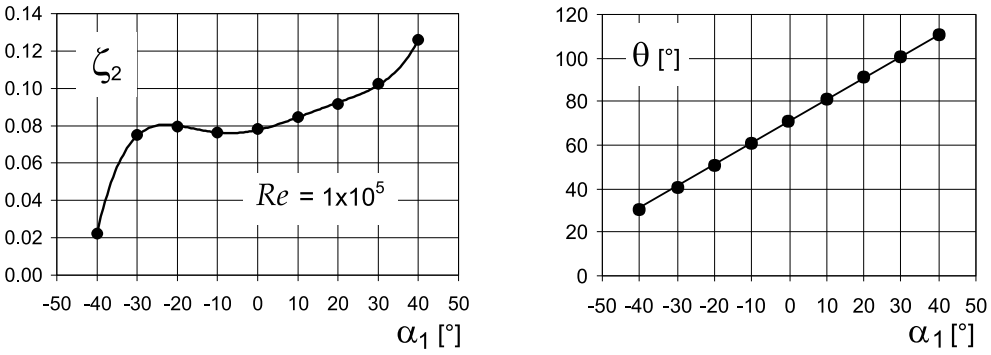

Figure 10. Loss coefficient ζ_2 and flow deflection θ as a function of angle of attack α_1, $\mathrm{Re} = 1 \cdot 10^5$, NACA profile A3K7 primary series, $t/c = 20\%$, $c/s = 1.1504$ and $\theta_c = 79^\circ$

6.1. Stator and rotor hydraulic loss coefficient

According to the above discussion of hydraulic loss sources, the stator and rotor loss coefficients are given by:

$$\zeta_{U_S} = \frac{1}{2}(\zeta_p + \zeta_{\mathrm{sec}}) \cdot \frac{C_2^2}{U_m^2}, \tag{21}$$

$$\zeta_{U_R} = \frac{1}{2}(\zeta_{p_R} + \zeta_{\mathrm{sec}_R}) \cdot \frac{W_3^2}{U_m^2} + \frac{1}{2}\zeta_{cl} \cdot \frac{U_p^2}{U_m^2}. \tag{22}$$

6.2. Hydraulic loss prediction

The stator and rotor experimental and theoretical hydraulic loss coefficients are compared in Figure 11. The following remarks can be stated:

- The theoretical results do not show a significant influence of the Reynolds number contrary to what was observed experimentally.
- There is not a good agreement between the theoretical and experimental results. The calculated ζ_{u_S} increases with the flow coefficient Φ, contrary to what was observed in the experiments.
- On the other hand, the theoretical ζ_{u_R} increases with the rotation speed n, just opposite to what was observed experimentally.

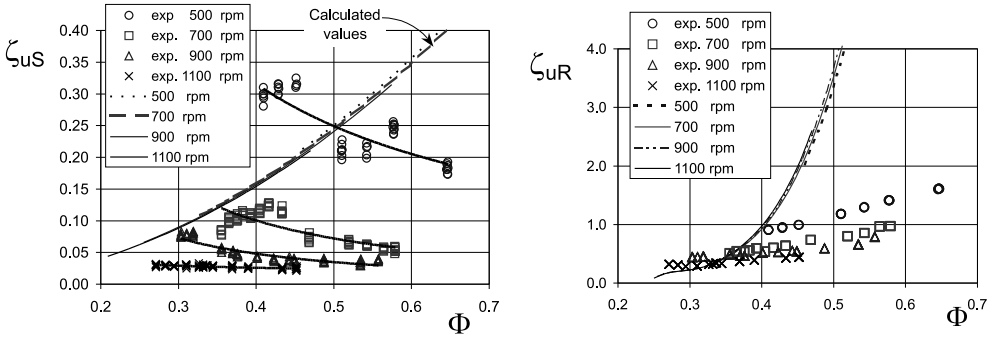

Figure 11. Comparison of theoretical and experimental hydraulic loss coefficients of the stator and rotor

These differences are explained as follow:

1. The numerical simulation conducted in the cascades was performed considering a smooth blade surface. A blade surface with a bigger roughness causes more turbulence; therefore, the profile flow losses should decrease faster as the Reynolds number increases.
2. The Reynolds number effect related to profile loss and the secondary losses was calculated from a 2D-cascade model. The complex 3D flow field developing close to the annulus and hub wall (horse-shoe vortex, clearance vortex, wakes *etc.*) should exhibit a higher Reynolds number influence.

7. Conclusions

The main conclusion of the stage dimensioning is: the smallest LSHAFT with high power-output is an action turbine. The optimum values of theoretical head coefficient ($\Psi_{\text{th}} = 2$) and flow coefficient ($\Phi = 0.577$) are maximal for an action turbine. Therefore, this turbine has the maximum head per stage, the smallest size, and the minimum number of stages.

With regard to the stage dimensioning in the cavitant regime, a 50% reaction turbine has a higher specific speed of cavitation, for the same relative span. Action and 50% reaction turbines, have the same size, since they have the same specific diameter of cavitation Λ_S. The beginning of the cavitation in a 50% reaction stage is more likely to occur at the rotor blades, while in the action stage, cavitation might begin at the stator blades. For an action stage, the selection of profiles with small factors of diffusion ($F_D \leq 0.25$) is required to decrease the turbine $\text{NPSH}_{\text{required}}$.

The experimental results on a small single stage 50% reaction turbine show a large influence of the Reynolds number on the turbine performance. The operation zone at the best efficiency point shows a strong variation with the rotation speed.

The performance analysis of a HAFT-HPWR requires a precise assessment of the Reynolds number influence on the deflection and hydraulic losses. Due to the complexity of the flow field developed in an axial turbine, such assessment should be based on a 3D CFD simulation. In this way, the hydraulic losses present in a HAFT-HPWR stage could be calculated directly, without using models and correlations.

Acknowledgements

The authors would like to thank the Embassy of France in Venezuela and the National Council of Scientific and Technological Research of Venezuela "CONICIT" for their financial support of this research.

References

[1] Harden B 1999 *Petroleum Engineer International* **72** (4) 59
[2] Horlock J H 1966 *Fluid Mechanics and Thermodynamics*, Butterworths, London
[3] Lakshminarayana B 1996 *Fluid Dynamics and Heat Transfer of Turbomachinery*, John Wiley & Sons, US
[4] Wilson D G 1987 *Proc. Instn. Mech. Engrs.* **201** (A4 111/87) 279
[5] Schoobeiri T and Abouelkheir M 1992 *J. Propulsion and Power* **8** (4) 823
[6] Holeski D E and Stewart W L 1964 *J. Engng. for Power, Trans. of the ASME*, Series A **86** 296

[7] Luu T S and Coulmy G 1990 *Principe et applications de la méthode de singularités à répartition discrétisée en hydro et aérodynamique*, Laboratoire d'Informatique pour la Mécanique et les Sciences de l'Ingénieur, France, No. 90–11
[8] CFX-4.2, AEA Technology plc. CFX International 8.19 Harwell, Didcot, Osfordshire OX11 0RA, United Kingdom, December 1997
[9] Sharma O P and Butler T L 1986 *Int. Gas Turbine and Aeroengine Congress and Exposition, ASME* **86-GT-228**, Dusseldorf, West Germany